# INFORMATION RETRIEVAL FROM HOLOGRAPHIC INTERFEROGRAMS - FUNDAMENTALS AND PROBLEMS*

Charles M. Vest

The University of Michigan

## ABSTRACT

Holographic interferograms can contain large amounts of information about flow and temperature fields. Their information content can be especially high because they can be viewed from many different directions. This multidirectionality, and fringe localization, add to the information contained in the fringe pattern if diffuse illumination is used. Additional information, and increased accuracy, can be obtained through the use of dual reference wave holography to add reference fringes or to effect discrete phase shift- or hetrodyne interferometry.

Automated analysis of fringes is possible if interferograms are of simple structure and good quality. However, in practice a large number practical problems can arise, so that a difficult image processing task results.

## INTRODUCTION

Realization of the potential of holographic interferometry as a scientific and engineering tool requires quantitative interpretation of holographic interferograms. The usefulness of the technique increases appreciably if data aquisition is rapid and processing of information contained in interferograms can be highly automated. This is particularly true in fields like fluid mechanics and combustion diagnostics where the fields to be measured may be quite complicated and changing rapidly with time. In this paper we consider the information contained in holographic interferograms of transparent media, discuss the basic concepts of quantitative interpretation of holographic interferograms, and pose the problems which must be addressed by those in involved in the development of automated systems for analysis of interference fringe patterns.

* This work was sponsored by the Army Research Office.

The process of applying holographic interferometry to fluid mechanics or combustion diagnostics, or for that matter any other scientific or industrial problem area, consists of the following ten steps:

1. Problem definition and goals
2. Apparatus and setup
3. Establishment of flow
4. Recording the hologram
5. Developing the hologram
6. Reconstruction
7. Viewing and storing
8. Analysis of fringes
9. Physical interpretation
10. Use of information

Holographic interferometry is defined as the interferometric comparison of two or more waves, at least one of which is holographically reconstructed. The composite of these two or more waves is referred to as a holographic interferogram. The term interferogram with no modifying adjective denotes a pattern of interference fringes recorded on photographic film or formed on a two-dimensional viewing screen, video device or the retina of the eye. It is assumed that the reader is familiar with the basic technology of holography.

This process in fact contains at least two feedback loops because physical interpretation generally feeds back to refinement of the apparatus and setup, and the use of information obtained from the holographic analysis usually feeds back to refinement of problem definition and goals.

In this paper we emphasize, in broad terms, the analysis of fringes and physical interpretation. However, the designer of an automated system for analysis of holographic interferograms must consider all eight of the above steps.

## FORMATION OF HOLOGRAPHIC INTERFEROGRAMS

In order to extract quantitative information from an interferogram, one must understand the process by which the interferogram was initially formed. This process is summarized in figure 1. A wave of coherent light enters, and propagates through, a test object which is the region of gas or liquid in which the phenomenon of interest occurs. The wavefronts of this coherent light are distorted, and possibly attenuated, by their interaction with the test object. The deformed wavefronts strike a holographic recording device where they are mixed with a reference wave in order to record a hologram. Most commonly this process is repeated twice, once with flow occurring and once with no flow, in order to form a two-exposure holographic interferogram. By illuminating such a two-exposure hologram the deformed an undeformed waves are simultaneously reconstructed. They enter some type of viewing or recording device to form an interferogram. This interferogram is the irradiance pattern of

the sum of the two coherent waves.

The basic information contained in a holographic interferogram is the distribution of relative phase of two waves encoded in a fringe pattern. However, there is additional information which may be of importance in quantitative evaluation. In many cases the fringes will be localized in space, and the apparent location of fringe localization provides some information about the field. Variation of background irradiance in the interferogram provides information about attenuation of the waves by the test object, and this attenuation constitutes spectroscopic data, i.e. it is related to the local absorbtivity of the fluid at the given wavelength of light. Knowledge of the precise direction of viewing of the interferogram is important information for quantitative evaluation.

To investigate evaluation of interferograms it generally is convenient to think in terms of ray optics, rather than wave fronts. Figure 2 is a general schematic diagram of the formation of an interferogram. This figure reminds us of three important facts about the formation of interferograms. First, rays are bent (refracted) as they pass through the active test object. Second, interference occurs only on the surface of the detector (film, viewing screen, video camera, retina, etc.). Third, knowledge of the imaging system such as its direction of view, location of image plane, and numerical aperture is required for proper interpretation.

In figure 2 we show two rays. The first (DFP') passed through the test section when no flow was occuring and its refractive index was a uniform value $n_o$ . The second ray (ACP') is bent by refraction as it passes through the nonuniform refractive index field $n(r,\phi)$ due to the flow of interest. These two rays meet and interfere on a detector surface at point P'. The imaging system is focused on the object plane indicated in the figure so that the interferogram appears to be an image of fringes in the plane containing point P within the test object. The optical path difference which can be determined from the fringe pattern is given by equation (1):

$$\widetilde{\Delta\Phi}(\rho,\theta) = \int_A^B n(r,\phi)ds + n_o(\overline{BC} - \overline{DE} - \overline{EF}) \qquad (1)$$

This expression for the optical pathlength difference can be thought of as a "pathlength transform" which must be inverted to determine the refractive index given measured values of the optical pathlength.

Fortunately in many cases refraction is sufficiently small that both rays contributing to the interference pattern at point

P'are very nearly straight lines passing in the same direction through the neighborhood of point P. We refer to this as the refractionless limit, a situation which usually can be assumed in aerodynamics if shocks are not present. In this case the path integral of equation (1) simplifies to the following line integral:

$$\overline{\Delta\Phi}(\rho,\theta) = \int_E^F [n(r,\phi) - n_o]dz. \qquad (2)$$

To evaluate an interferogram we must carry out the following steps:

1. Measure the location of the fringes and convert them to a phase distribution.

2. Invert an equation such as (1) or (2) above to convert the phase distribution to a refractive index distribution within the fluid.

3. Convert the distribution of refractive index to a distribution of some fluid property (for example mass density).

4. Possibly convert the distribution of this fluid property to a derived property (such as velocity of a compressible flow).

Consider the simplest case of a boundary layer like flow over a flat surface. The refraction effects are negligible, the flow and refractive index fields have essentially no variation in the z direction, and the holographic object wave is a plane wave such that all optical rays are essentially straight lines parallel to the surface. In this case, which is shown schematically in figure 3, fringes are nonlocalized, i.e. they can be observed in any plane normal to the z axis. The fringe pattern is shown schematically in this figure. Fringe numbers are assigned as indicated and as shown in equations (3) and (4), the determination of the refractive index distribution is quite simple.

$$\overline{\Delta\Phi}(y) = \int_0^L [n(y) - n_o]dz$$

$$= [n(y) - n_o]L = N\lambda \qquad (3)$$

$$n(y) - n_o = N\lambda/L \qquad (4)$$

Now suppose that a diffusing screen, for example a plate of ground or opalized glass is placed behind the test section as shown in figure 4. Three things will be different in this

interferogram than in that considered above. First, the fringe pattern will be viewable from a variety of directions by the unaided eye or a camera. Second, the fringes will appear to be localized in space, as indicated in the figure. This means that the eye or other viewing instrument must be focused on the region of apparent localization of the fringes. For information about the phenonmenon of fringe localization, see reference 1. Third, the interferogram will now contain laser speckle. That is, the fringes will be a modulated speckle pattern.

To first approximation, the fringes will be localized in the region given by equation (5):

$$z_l = \frac{\int_{-\infty}^{\infty} \frac{\partial}{\partial y}[n(y) - n_o]z\,dz}{\int_{-\infty}^{\infty} \frac{\partial}{\partial y}[n(y) - n_o]\,dz} \qquad (5)$$

This means that the fringes appear to the observer to be at the centroid of the normal transverse gradient of the field. An in-depth analysis of this type of fringe localization is given in reference 2. In the case of reasonably simple two- or three-dimensional fields, this localization gives the observer some qualitative understanding of the structure of the distribution. Decker (ref. 3) has shown that fringe localization in rapid-pulsed interferograms of complicated compressible flows leads to a very useful flow visualization technique.

An important technique for increasing the information content of an interferogram is to use two reference waves when forming the hologram as shown in figure 5. Reference wave R1 is used to record the first holographic exposure (no flow). Reference wave R2 is used to make the second holographic recording (with flow). After the hologram is developed if reconstruction waves identical to R1 and R2 are used, the interferogram will appear precisely as in figure 3(b). However, if we tilt the reconstruction wave R2 slightly relative to R1 we may form a pattern such as that in figure 5(b). Knowing the amount and direction of tilt, we will know the sign of the gradient of refractive index change (ref 9). This sign cannot be determined from the interferogram in figure 3(b) unless we understand the physics of the flow.

The use of dual reference beams also enables one to apply <u>discrete phase shift interferometry</u> (or quasiheterodyne interferometry). In this case the reconstruction waves are identical to R1 and R2 so that the interferogram appears as in figure 3(b). The irradiance at any point (x,y) can be written as

$$I_1(x,y) = I_o[1 + \cos(\bar{\Delta}\Phi)] \qquad (6)$$

Now suppose that we sequentially introduce a phase shift first of $+120^{\circ}$ and then of $-120^{\circ}$ into one of the reconstuction waves, say R1. This has the effect of laterally shifting the position of each fringe by a known amount, or, equivalently the irradiance at the same point (x,y) is given by equations (7) and (8), respectively.

$$I_2(x,y) = I_o[1 - \cos(\Delta\bar{\Phi}) - \sqrt{3}\cos(\Delta\bar{\Phi})] \quad (7)$$

$$I_3(x,y) = I_o[1 - \cos(\Delta\bar{\Phi}) + \sqrt{3}\cos(\Delta\bar{\Phi})] \quad (8)$$

By combining equations (6) - (8) it follows that:

$$(1/\sqrt{3})\tan(\Delta\bar{\Phi}) = (I_3 - I_2)/(2I_1 - I_2 - I_3) \quad (9)$$

Thus, given these three irradiance values at a point one can calculate the corresponding phase difference. This technique has several advantages. First, it is naturally adapted to the use of solid-state array video cameras and digital data processing. Second, problems of sign ambiguity can be overcome. Third, the distribution of phase or optical pathlength can be calculated with great accuracy, regardless of variations of background irradiance. Useful papers on the topic include those of Dandliker, et. al (ref 4.) and Hariharan, et. al. (ref. 5).

A third two-reference wave technique based on analog rather than digital electronic processing is heterodyne holographic interferometry. Two separate holographic exposures are recorded as above. The resulting hologram is illuminated with reconstruction waves idential to R1 and R2. However, one of these recostruction waves is shifted in temporal frequency by an amount $\Omega$. The resultant time-varying irradiance at a point (x,y) is given by equation (10).

$$I(x,y,t) = I_o[1 + \cos(\Omega t + \Delta\bar{\Phi})] \quad (10)$$

From equation (10) it can be seen that the desired optical pathlength difference appears as a phase of a sinusoidal irradiance which can be detected by a sensor such as a photomultiplier tube or a photodiode because the frequency is sufficiently low (typically 100k Hz). The resultant signal can be fed into an electronic processor such as a phase meter or lock-in amplifier to determine the phase at any point. This technique is capable of high sensitivity up to the order of $\lambda/1000$, and the relative sign of the shift in phase, or equivalently optical pathlength, can be determined across the entire field. Figure 6 is a diagram of a heterodyne system used for interferometric measurements of temperature distributions in gasses (ref. 6). A detailed discussion of the theory and technology of heterodyne holographic interferometry is given in the review article by Dandliker (ref. 7).

## MULTIDIRECTIONAL INTERFEROMETRY

It was noted above that if the test section is back illuminated with a diffusing screen a holographic interferogram can be viewed from many different directions. This multidirectional property is unique to holographic interferometry and is its richest source of information content. Other ways of creating multidirectional interferograms are indicated in figure 7. These include the use of phase gratings to break an incoming plane wave into a number of plane waves traveling in various directions through the test section, the use of multiple collimated beams, and the use of a fixed object wave through which the object itself rotates. Regardless of which technique is used to record the multidirectional interferograms, one obtains measurements of line integrals of the refractive index distribution corresponding to each direction of view. This is indicated in figure 8. With reference to this figure, the optical pathlength difference along a typical line through the test object can be written as:

$$\Delta\bar{\Psi}(p,\theta) = \int\int f(r,\phi)\delta[p - r\sin(\phi - \theta)]dxdy$$

$$= \lambda N(p,\theta) \qquad (11)$$

Where $f(r,\phi) = n(r,\phi) - n_o$, $\delta$ is the Dirac delta function, $\lambda$ is the wavelength of light and $N(p,\theta)$ is the fringe order number at point P. The set of all line integrals (eq. (11)) through a plane in the test region is know as the Radon transform (ref. 8). Reconstrution of the desired distribution $f(r,\phi)$ is accomplished by computing the inverse Radon transform:

$$f(r,\phi) = \frac{1}{2\pi^2}\int_{-\frac{\pi}{2}}^{\frac{\pi}{2}} d\theta \int_{-\infty}^{\infty} \frac{(\partial N/\partial p)dp}{r\sin(\phi - \theta) - p} \qquad (12)$$

Computation of such reconstruction from projections is known as <u>computed tomography</u>. Because of the applicability of this computational technique to many scientific and engineering fields, predominantly x-ray and nuclear medicine, a very large literature exists, and is reviewed in reference 8. Examples of the combination of multidirectional holographic interferometry and computed tomography to fluid mechanics and heat transfer are given in references 9 and 10, respectively. An application to helicoptor rotor aerodynamics, in which data are gathered using a configuration like figure 7(d) is given by Kittleson (ref. 11). A proposed extension of this technique to cases in which refraction causes appreciable bending of the probing optical rays is given in reference 12.

## RELATION OF REFRACTIVE INDEX TO OTHER PHYSICAL PROPERTIES

Once an interferogram has been analyzed to determine a spatial distribution of refractive index, this must in turn be related to the physical property of interest. Although this is a very important step in information retrieval from interferograms, we will not review this topic in detail here. The reader may refer to reference 1 for further information. However, we note that in aerodynamics the desired relation is quite simple, namely the Gladstone-Dale relation

$$n - 1 = K\rho \tag{13}$$

Where K is the Gladstone-Dale constant of the gas and $\rho$ is its density. In some cases another derived property can in turn be computed from knowledge of the distribution density. For example, if a compressible gas flow can be considered essentially isentropic the velocity can be computed using equation (14).

$$\frac{v}{c_t} = \left[ \frac{2}{\gamma - 1} \left( 1 - \left( \frac{\rho}{\rho_t} \right)^{\gamma - 1} \right) \right]^{\frac{1}{2}} \tag{14}$$

Where $c_t$ and $\rho_t$ are the speed of sound and density at stagnation conditions, respectively, and $\gamma$ is the ratio of specific heats of the gas. In reference 13 distributions of Mach number in a transonic flow, determined in this manner, are presented.

## ANALYSIS OF FRINGE PATTERNS

Having described the general information content of holographic interferograms, we now turn to the problems associated with direct analysis of fringe patterns to determine the distribution of fringe order across an interferogram. Ideally this shold be a reasonably straightforward task. Consider the interferogram in figure 9. The broad region around the periphery of the pattern serves as a reference region in which no change has occured, so it is assigned the fringe order number N = 0. The center of the first dark fringe is assigned the value N = 0.5, the center of the next bright fringe is N = 1.0, etc. It should be a reasonably simple matter to digitally preform the assignment of fringe order number in this manner, and automation should be possible. However, there are a few difficulties. First, unless the operator understands the physics of the problem there is no way of knowing whether the fringe order numbers are positive or negative. Second, if the fringes are rather broad there may be some difficulty identifying their precise centers, and knowing values just at the fringe centers may not give a high enough density of data to analyze the physical properties of interest. Also, the fringes may be so

finely spaced that resolving them is difficult. Nonetheless, with an ideal interferogram as in figure 9 a high degree of automation should be possible. Unfortunately, in many experiments in fluid mechanics and combustion the interferograms may be far less than ideal. Figure 10 represents an interferogram exhibiting many of the problems that can occur in practice. Among difficulties that make analysis difficult, especially automated analysis, are the following:

1. Discontinuous fringes
2. Extraneous fringes
3. Broad, "cloud-like" fringes
4. No fringe closure
5. Very closely spaced fringes
6. No region of known reference value
7. Inadvertent wedge fringes
8. Unknown sign of fringe order
9. Nonuniform background irradiance
10. Caustics due to refraction and diffraction
11. Data blocked by opaque objects
12. Diffraction by solid boundaries
13. Laser speckle

Some of these difficulties can be eliminated, or alieviated by the use of the various two-reference-wave techniques discussed above. Most, however are present regardless of how the interferogram is recorded. Some of these factors lead inevitably to errors in results, and some generally will require human interpretation based on experience and/or knowledge of the physics of the problem. Most are quite likely to cause serious difficulties if one attempts to fully automate the readout process.

With the warning of these difficulties in mind, we now consider the basic tasks which must be undertaken by readout systems which are automated to some extent. It is convenient to divide the problem into two categories: Local analysis (i.e. along single line scans), and global analysis (i.e. over a two dimensional interferogram). The local problem can be approached by reasonably classical data analysis techniques. The global problem is basically one of digital image processing.

Line scan data are usually obtained by one of three means: scanning with a photodetector or microdensitometer, scanning with a video camera, or recording the output of a solid-state photodetector array. In any of these cases the data to be computationally analyzed consist of a vector of irradiance values. Because of problems such as nonuniform background irradiance, laser speckle, and variable fringe spacing, a simple approach of finding the maxima and minima in this spector of irradiance values generally is quite insufficient. One approach,

which is particularly suited to widely spaced fringes, is to interpolate, generally through the use of curve fitting. A variety of spline functions and polynomials have been used for this purpose by various workers. An effective but computationally-intensive approach is nonlinear regression analysis to fit digitized irradiance data to the following function which represents the general form of a fringe pattern:

$$I(x) = b(x) + a(x) \cos[\Delta\bar{\phi}(x)] \qquad (15)$$

In equation (15) $b(x)$, $a(x)$, $\Delta\bar{\phi}(x)$ represent the background irradiance, the fringe amplitude, and the unknown optical pathlength difference, respectively. Each of these can be represented by a polynomial or other functional representation including unknown constants. By nonlinear regression analysis the unknown constants can be determined to fit the data optimally with respect to some criterion. Figure 11 shows raw data containing a lot of noise (laser speckle) and a curve of the form of equation (15) fitted to it by regression analysis (ref. 14).

Because of the basically periodic nature of interference fringes the Fourier transform can be used to analyze data accumulated by a line scan. The spatial-frequency spectrum of the irradiance data is computed using a fast Fourier transform algorithm. Some filtering, for example by the use of a Hanning window, and separation from carrier frequencies are generally required. The appropriately filtered spectrum can then be inverted by an FFT routine to determine the distribution of phase (optical pathlength difference). A discussion of this approach and examples of its use with real interferograms is presented in reference 15.

Two basic issues immediately confront the designer of a system for global (two-dimensional) analysis of interferograms. The first is the basic strategy, i.e. to consider the interferogram to be a collection of individual line scans, or to connect and track each fringe. The second is to determine the extent of automation, i.e. what, if any, degree of interaction with a knowledgeable operator is permissable. An example of a highly interactive approach is that given by Funnell (ref. 16), and an example of a quite highly automated system is that of Becker, et al (ref. 17). Systems of intermediate degrees of automation are described in detail in the paper by Cline, et. al. (ref. 18) the thesis of Choudry (ref. 19).

Generally the tasks to be performed by an automated fringe read out system constitutes some subset of the following:

1. Pre-processing
   - Digitization
   - Filtering

Contrast enhancement
Smoothing
Boundary specification

2. Fringe Tracking and Interpretation
   Segmentation
   Fringe edge detection
   Detection of obstacles
   Detection of fringe intersections
   Fringe numbering
   Noise reduction
   Polynomial fitting
   Operator interaction

3. Data Display
   Isometric representation
   Wire frame
   Contour plot
   Shaded surfaces

Details of systems developed by various workers are presented elsewhere in these proceedings.

It should be noted that there are some applications in which a high degree of automation is possible because the required information is modest. For example in applications to nondestructive testing the presence of a flaw may be made known simply by a locally high density of fringes. A fully automated system for this case is described in reference 20.

## CLOSING

It is clear that a large amount of information about an experiment in fluid mechanics or combustion diagnostics can be encoded in a holographic interferogram. The concepts and basic means for interpreting fringe order data are well known, although in practice serious computational problems may be encountered. Perhaps the most pressing problems in the field is that addressed in this workshop, namely the automated analysis of interferograms to provide fringe order data. In many applications this presents a formidible image processing problem. Furthermore, in most applications significant interaction with a knowledgeable operator is likely to be required. As a closing comment I would like to note that the problem of automated fringe analysis may be ripe for application of concepts of artficial intelligence, particularly expert systems.

## REFERENCES


1. Vest, C. M.: Holographic Interferometry. John Wiley & Sons, Inc., 1979.

2. Schumann, W.: Fringe Localization in Holographic Interferometry in the Case of a Transparent Object with a Nonuniformly Varying Indes of Refraction. Opt. Lett., vol. 7, Dec. 1982, pp. 119-121.

3. Decker, A. J.: Holographic Flow Visualization of Time-Varying Shock Waves. Appl. Opt., vol. 20, 15 Dec., 1981, pp. 3120-3127.

4. Dandliker, R.; Thalmann, R.; and Willemin, J.-F.: Fringe Interpolation by Two-Reference-Beam Holographic Interferometry: Reducing Sensitivity to Hologram Misalignment. Opt. Commun., vol. 42, 1 Aug., 1982, pp. 301-306.

5. Hariharan, P.; Oreb, B. F., and Brown, N.: A Digital Phase-Measurement System for Real-Time Holographic Interferometry. Opt. Commun., vol. 41, 15 May, 1982, pp. 393-396.

6. Farrell, P. V.; Springer, G. S.; and Vest, C. M.: Heterodyne Holographic Interferometry: Concentration and Temperature Measurements in Gas Mixtures. Appl. Opt., vol. 21, 1 May, 1982, pp. 1624-1627.

7. Dandliker, R.: Heterodyne Holographic Interferometry, in Wolf, E. (Ed.), Progress in Optics Vol. XVII. North - Holland, 1980, pp. 1-84.

8. Deans, S. R.: The Radon Transform and Some of Its Applications. John Wiley & Sons, Inc., 1983.

9. Zien, T.-F.; Ragsdale, W. C.; and Srring, W. C.: Quantitative Determination of Three-Dimensional Density Field by Holographic Interferometry. AIAA J., vol. 13, 1975, pp. 841-842.

10. Sweeney, D. W.; and Vest, C. M.: Measurement of Three-Dimensional Temperature Fields Above Heated Surfaces by Holographic Interferometry. Int. J. Heat Mass Transfer, vol. 17, December, 1974, pp. 1443-1454.

11. Kittleson, J.: A Holographic Interferometry Technique for Measuring Transonic Flow Near a Rotor Blade. NASA TN84405, 1983.

12. Cha, S.; and Vest, C. M.: Tomographic Reconstruction of Strongly Refracting Fields and its Application to Interferometric Measurement of Boundary Layers. Appl. Opt., vol. 20, 15 Aug. 1981, pp. 2787-2794.

13. Johnson, D. A.; and Bachalo, W. D.: Transonic Flow About a Two-Dimensional Airfoil - Inviscid and Turbulent Flow Properties. Paper 78-117, AIAA 11th Fluid and Plasma Dynamics Conference, Seattle, WA, July 1978.

14. Schemm, J. B., and Vest, C. M.: Fringe Pattern Recognition and Interpolation Using Nonlinear Regression Analysis. Appl. Opt., vol. 22, 15 Sept., 1983, pp. 2850-2853.

15. Fakeda, M.; Hideki, I.; and Kobayoski, S.: Fourier-Transform Method of Fringe Pattern Analysis for Computer-BAsed Topography and Interferometry. J. Opt. Soc. Am., vol. 27, 1 January, 1982, pp. 156-160.

16. Funnell, W. R.: Image Processing Applied to the Interactive Analysis of Interferometric Fringes. Appl. Opt., vol. 20, 15 Sept., 1981, pp. 3245-3250.

17. Becker, F.; Meier, G. E.; and Wegner, H.: Automatic Evaluation of Interferograms. Proc. SPIE, vol. 359, 1982, pp. 386-393.

18. Cline, H. E.; Holik, A. S.; and Lorensen, W. E.: Computer-Aided Surface Reconstruction of Interference Contour. Appl. Opt., vol. 21, 15 Dec., 1982, pp. 4481-4488.

19. Choudry, A.: Automated Digital Processing of Interferograms. Doctoral Dissertation, Technische Hogeschool, Delft, 1982.

20. Tichenor, D. A.; and Madsen, V. P.: Computer Analysis of Holographic Interferograms for Nondestructive Testing. Opt. Engin. vol. 18, 1979, pp. 469-472.

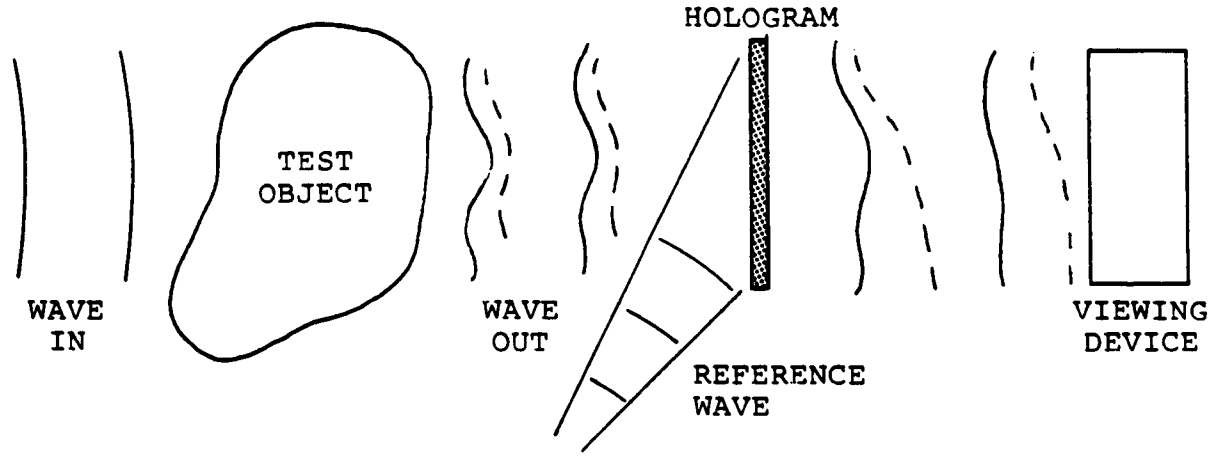


**Figure 1. Holographic interferometry of transparent media.**

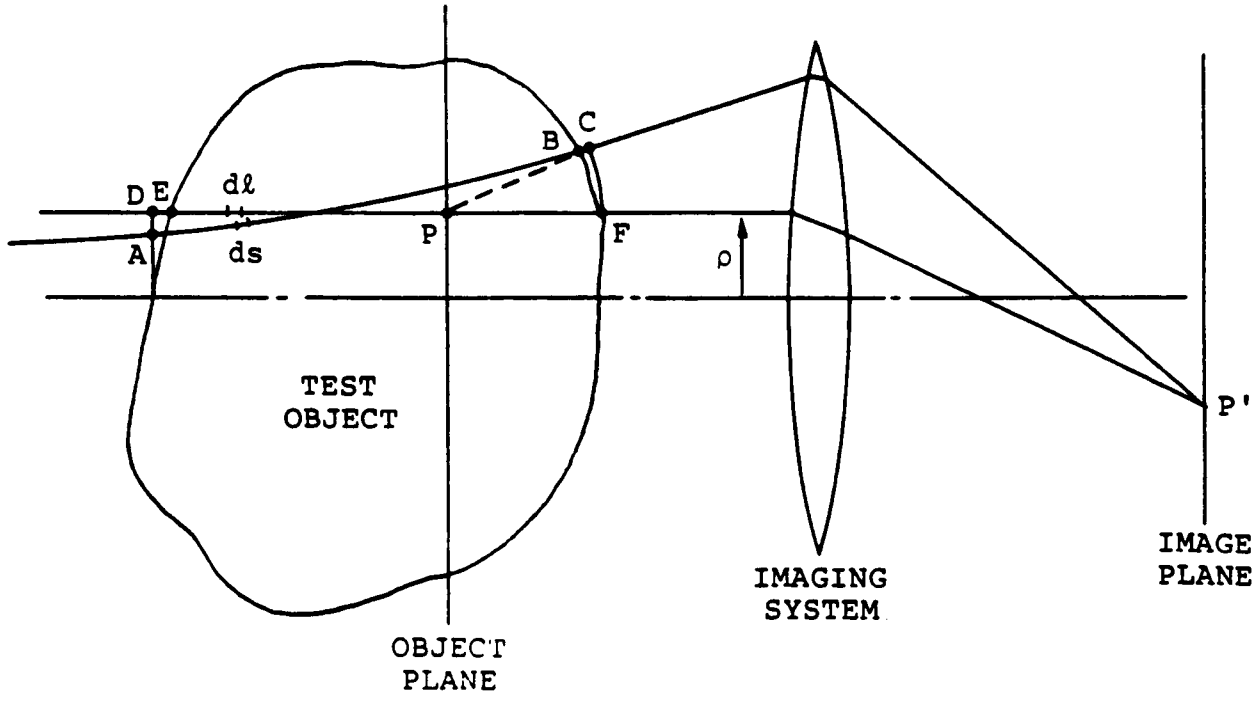


**Figure 2. Ray optics of interferorgram formation.**

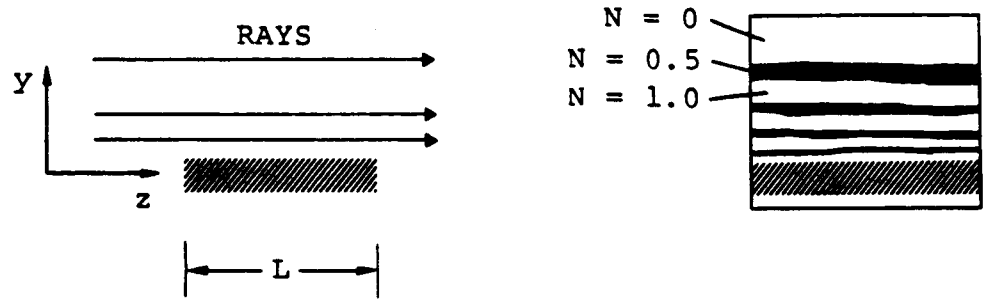


(a) (b)

Figure 3. Formation of an interferogram with a plane object wave. The fringes are not localized.

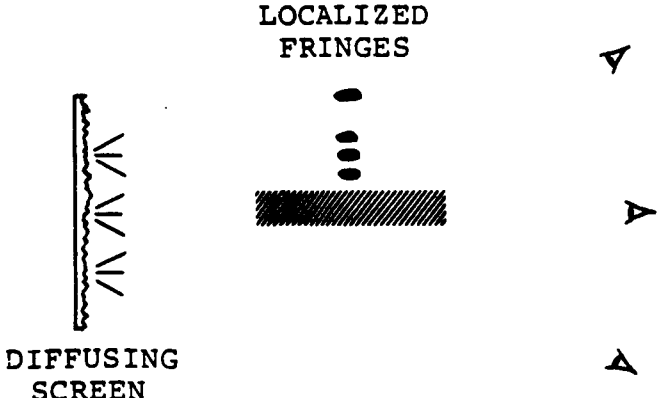


Figure 4. Formation of a holographic interferogram with diffuse illumination. The fringes appear to be localized, and they can be viewed from many different directions.

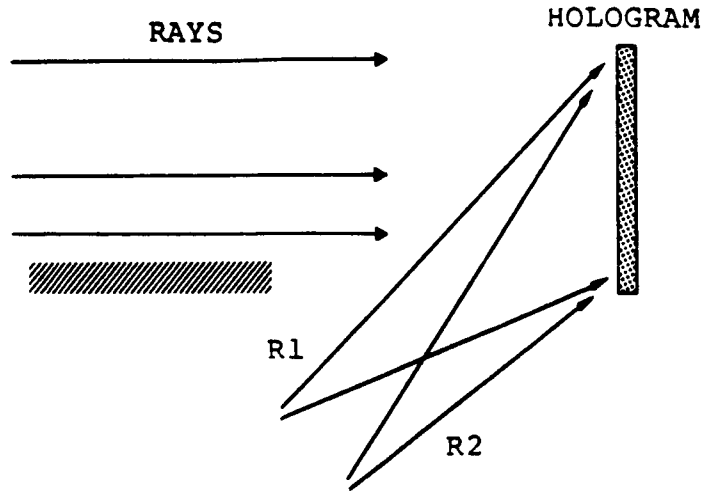


(a)

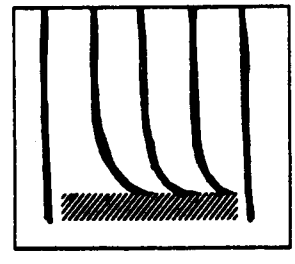

(b)

Figure 5. Two-reference wave holographic interferometry. (a) Separate waves are used to record each exposure; both are used for reconstruction. (b) Reference fringes can be introduced by tilting one reconstruction wave.

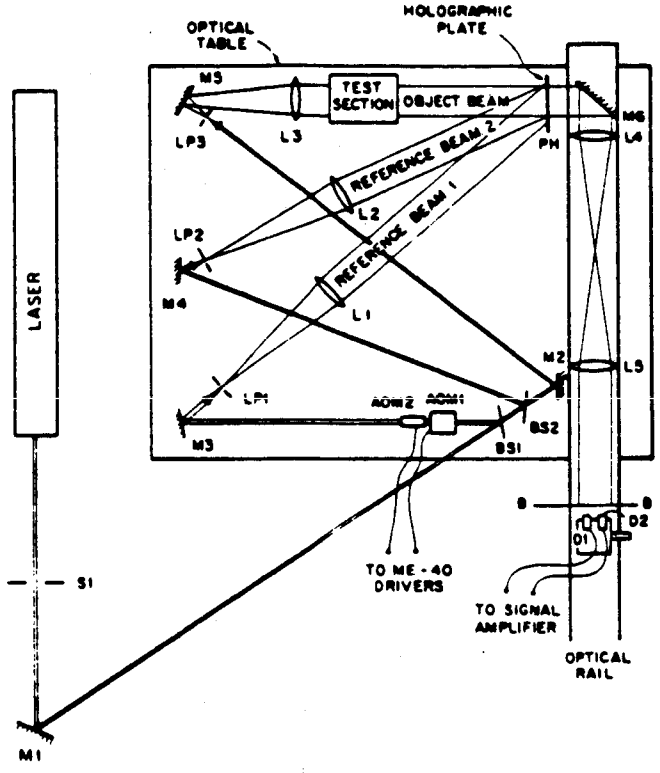


Figure 6. Heterodyne holographic inteferometer.

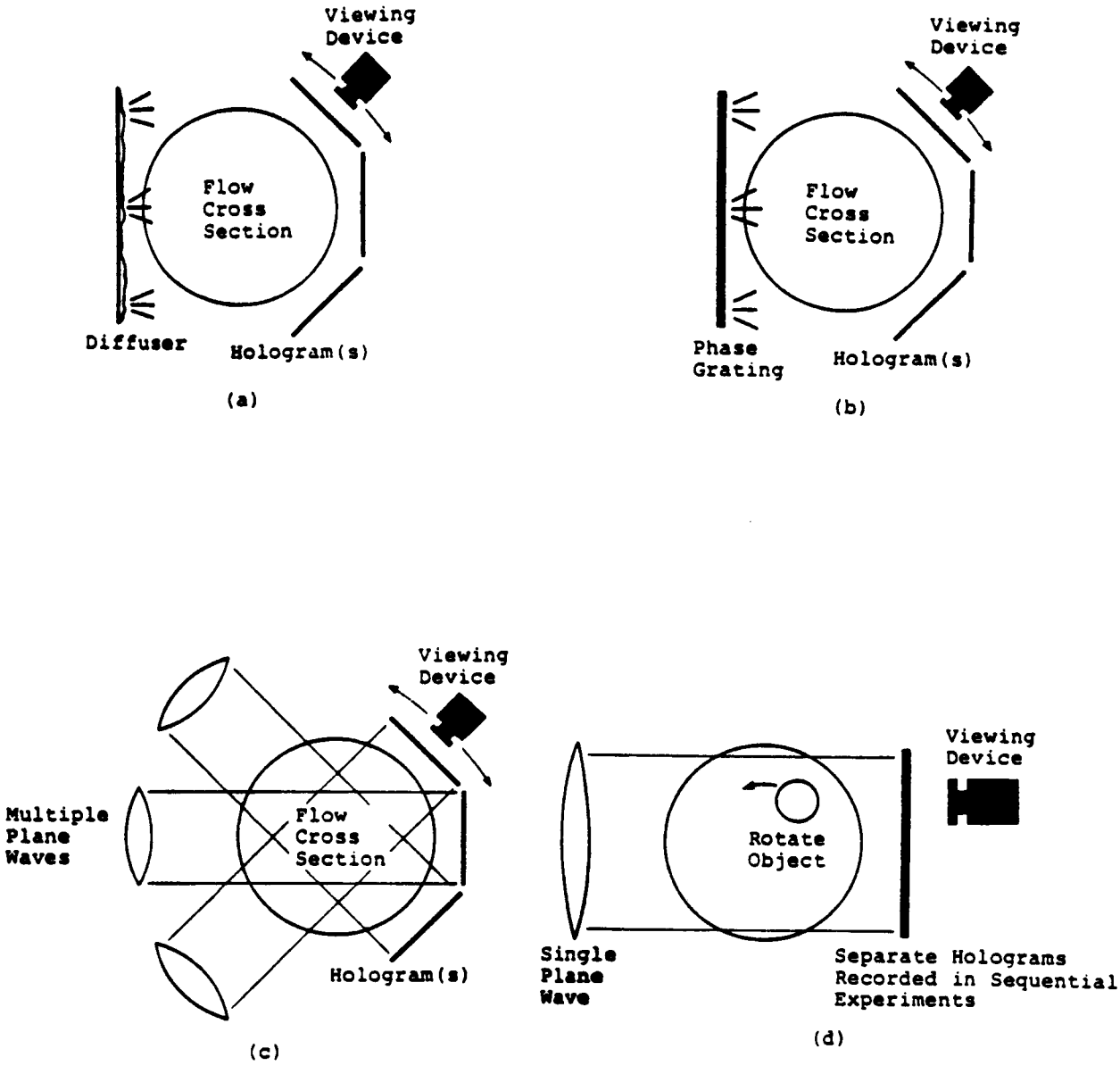


Figure 7. Techniques for recording multidirectional holographic intrferograms.

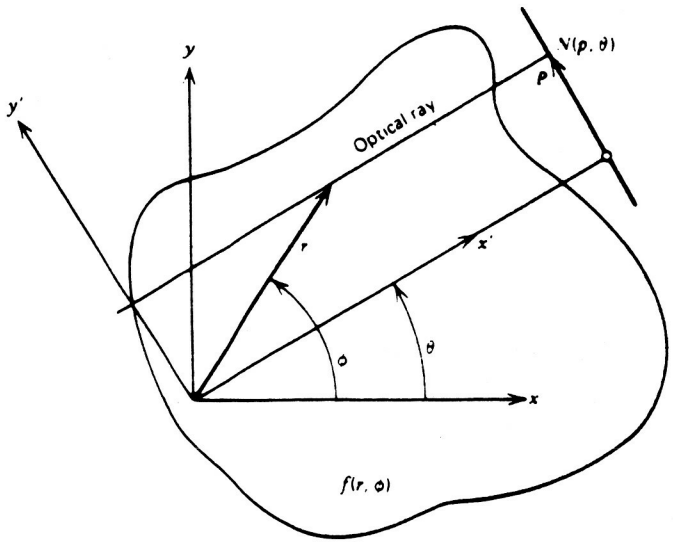


Figure 8. Nomenclature for multidirectional interferometry.

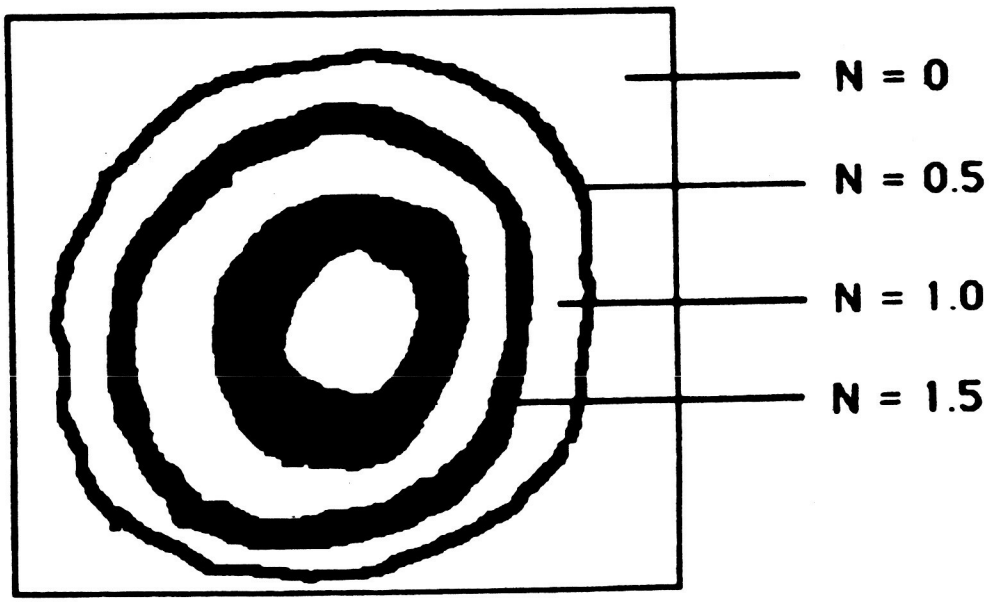


Figure 9. Ideal interferogram.

Figure 10. Interferogram exhibiting laser speckle and other problems encountered in practice.

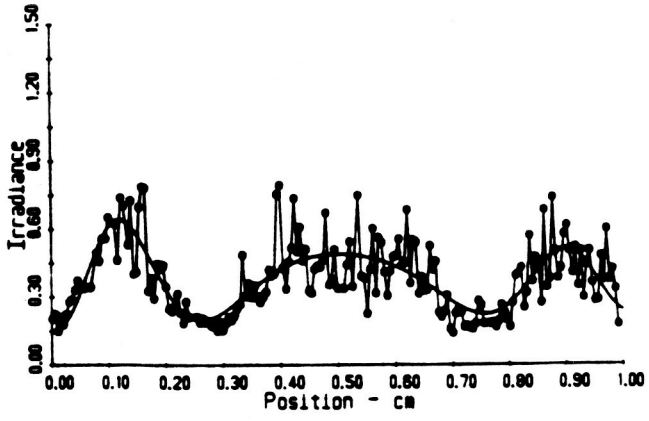


Figure 11. Irradiance distribution from real interferogram containing speckle noise. The solid curve was determined from these data by nonlinear regression analysis.